Volumetric Properties of Pressure-Transmitting Fluids up to 350 MPa: Water, Ethanol, Ethylene Glycol, Propylene Glycol, Castor Oil, Silicon Oil, and Some of Their Binary Mixture

Bérengère Guignon,* Cristina Aparicio,† and Pedro D. Sanz‡

MALTA Consolider Team, Department of Engineering, Instituto del Frío, Instituto de Ciencia y Tecnología de los Alimentos y Nutrición (C.S.I.C.), C/José Antonio Novais 10, 28040 Madrid, Spain

High-pressure processes carried at low or high temperatures often require the use of pressure-transmitting fluids (PTFs) other than water. Optimization of those processes involves their numerical simulation. The mathematical model used for that purpose depends on the physical properties of the PTF which vary with both pressure and temperature. The purpose of this work was to study the volumetric properties of different PTFs and evaluate how different they were from those of water. Castor oil, silicon oil, propylene glycol, ethylene glycol, and ethanol specific volumes were determined between (273.15 and 313.15) K and up to 350 MPa, individually and in a mixture with water or ethanol. The thermal expansion coefficient and the isothermal compressibility were derived from those measurements. The volumetric properties of all of the PTFs showed a behavior with pressure and temperature different from that of water. Specific volumes of the binary mixtures of these fluids were predicted within 3 % on a relative basis. These results will be useful in particular for modeling and to select the PTF that best fits with a given application.

Introduction

High hydrostatic pressure applied to food is emerging as an innovative soft technology for conservation and creation of new products regarding texture and functionality.[40,26] The equipments work by batch or in a semicontinuous way. Thus, there is an important challenge concerning the design and development of continuous equipment for food industrial production. These tasks and also that of process optimization involve the knowledge of material physical properties under high pressure. These are, in particular, the volumetric properties of food and of the pressure-transmitting fluid (PTF). The density, ρ, or its inverse value, namely, specific volume, v, the thermal expansion coefficient, α, and the isothermal compressibility coefficient, k_T, are necessary to calculate heat transfers and convective movement in liquids (Navier−Stokes equations) and to assess volume changes with pressure and temperature. The temperature distribution in a food product and the associated microbial inactivation can be predicted from those calculations. However, these properties are seldom available under high pressure, and in fact, this is a quite recent research topic.[19,10,41] When no data exist, the only solution is then to approximate food properties from those of water.[3,22] This is a relatively easy task because water is the main component of much food and its properties are known in a wide range of temperature and pressure. Moreover, water is the principal PTF used in the food industry. Thus, these approximated properties can be initially helpful to evaluate treatment uniformity, for example, but with a limited predictive power.

Besides, the high-pressure technology in food is developing toward new processes by combining pressure with temperature, for example, freezing and sterilization. These processes involve PTFs other than water. For instance, processes at subzero temperatures require the use of PTFs with a freezing point below 248.15 K (e.g., glycols). Sterilization at high pressure should be enhanced by using a PTF with a higher compression heating than water (e.g., silicon oil).[2,28,42] The same lack of data on volumetric properties for PTFs as for food under pressure is observed. Data on organic and inorganic liquid compounds can be found at high pressure, but they mostly concern compounds used for chemical industry applications or studied in the physics of the universe.[37] In contrast to food composition, the PTF usually contains a lower amount of or no water. In such cases, approximations from water properties may be hazardous or even impossible. The main objective of this work is to provide data on volumetric properties of PTFs. These data will be compared to those of water and between each other to characterize each PTF. An estimation of PTF mixture properties from those of its components will also be tested.

Materials and Experimental Procedure

Samples. Volumetric properties were studied for different PTFs habitually used at low temperatures whose composition is indicated in Table 1. The components of those PTFs were deionized water (W), ethanol (E), propylene glycol (PG), ethylene glycol (EG), castor oil (CO), and silicon oil (SO). Measurements were performed on the PTFs in the same conditions as they are used in high-pressure equipment, that is, without degassing. Thus, the volumetric properties given in this paper should be regarded as "apparent" properties. Nonetheless, it will be seen from comparison with data from other authors that the difference with "true" properties can be considered negligible for engineering purposes.

Experimental Setup. The specific volume at atmospheric pressure has been obtained as the inverse of the density which was measured with a densimeter (density meter DMA5000,

* Corresponding author. Tel.: +34 91 544 56 07; fax: +34 91 549 36 27. E-mail address: bguignon@if.csic.es (B. Guignon).
† E-mail: caparicio@if.csic.es.
‡ E-mail: psanz@if.csic.es.

10.1021/je9010568
Published on Web 02/23/2010

Table 1. Composition of the PTFs Studied

mix	supplier	ϕ_1	ref	abbreviation
ethanol	JVF 96°, Betamadrileño S.L., Spain (contains 0.1 % w/v benzalconium chloride)	1.00	6	E
ethanol (1) + water (2)		0.50	46	E+W
propylene glycol	PRS 99.5 %, Panreac, Spain	1.00	7	PG
propylene glycol (1) + water (2)		0.55	25	PG+W
ethylene glycol	Panreac, Spain	1.00	6	EG
ethylene glycol (1) + water (2)		0.75	20	EG+W
ethylene glycol (1) + etanol (2)		0.80	15	EG+E
castor oil	Panreac, Spain	1.00		CO
castor oil (1) + ethanol (2)		0.15	33	CO+E
silicon oil	SilOil Typ M40.165.10, Peter Huber Kältemaschinenbau GmbH, Germany; kinematic viscosity of 10^{-5} $m^2 \cdot s^{-1}$ at 298.15 K	1.00	8	SO

Anton-Paar GmbH, Graz, Austria). This densimeter allows for measuring densities between (0 and 3000) $kg \cdot m^{-3}$ at temperatures between (273.15 and 363.15) K. The standard uncertainties were 0.002 K for temperature and $6 \cdot 10^{-8}$ $m^3 \cdot kg^{-1}$ for specific volume. The repeatability between triplicates was about ± 0.003 K for temperature and ± 1.1 10^{-7} $m^3 \cdot kg^{-1}$ for specific volume at atmospheric pressure.

The specific volume at high pressure has been determined from direct measurements as a function of pressure at constant temperature. The device used may be classified as a variable-volume piezometer with a solid-piston volumeter. It was designed and constructed at the Institute of High Pressure Physics in Warsaw (Poland) by Unipress. The standard uncertainty on volume change measured by this device was calculated to be around $1.3 \cdot 10^{-7}$ $m^3 \cdot kg^{-1}$. It consists of a stainless steel cylindrical sample holder with a mobile piston inside. The piston is provided on its top with a ferromagnetic core, and its displacements can be monitored from a linear variable differential transformer. The whole system is assembled on the upper plug of a high-pressure vessel connected to a hydraulic pump (high pressure pump 700 MPa type U111, Unipress, Warsaw, Poland). A full description of each part of the equipment can be found in ref 9 for the volumetric device and in ref 8 for the high-pressure equipment (U111, Institute of High Pressure Physics, Warsaw, Poland).

Procedure for Measurements under High Pressure. The sample holder was filled with about 17 mL of the studied PTF, purged to evacuate air bubbles, and weighted (m) after tare. It was placed in the vessel and immerged in a thermostatic bath (Haake F3-K, Fisons Instruments, Karlsruhe, Germany); it took coarsely between half an hour and one hour to bring the sample to the required temperature. The temperature was checked by a T-type thermocouple (combined standard uncertainty 0.07 K) in contact with the bottom part of the sample holder. Then pressure was slowly increased by 50 MPa steps up to 350 MPa, waiting for more than 10 min for temperature equilibration between each pressure increase. Pressure was measured in the capillary connecting the intensifier with the vessel by a strain gauge transducer (type EBM 6045 V-0-10 GmbH, KGT Kramer, Dortmund, Germany; combined standard uncertainty 0.04 MPa). The temperature, pressure, and position of the piston were recorded every 0.5 s by using a data acquisition system (DC100 Data Collector Yokogawa, Tokyo, Japan). The data recorded during 1 min after temperature equilibration at each pressure were averaged to give the final result. The repeatability of these measurements (p, T, position of piston) was about ± 0.03 K for temperature, ± 0.1 MPa for pressure, and $\pm 2 \cdot 10^{-6}$ m (i.e., $\pm 9 \cdot 10^{-10}$ $m^3 \cdot kg^{-1}$) for the position of piston, respectively. When the maximal working pressure of 350 MPa was reached, the pressure was released, and the sample holder was newly weighted to control that neither a leak of sample nor contamination of it with silicon oil occurred. The complete procedure was repeated at least three times for each PTF.

The specific volume at pressure p was:

$$v(p) = v_0 + \frac{\Delta V(p)}{m} + \Delta v_{\text{calib}} \tag{1}$$

where v_0 is the specific volume of the sample at atmospheric pressure; $\Delta V(p) = S\Delta x(p)$ was the sample volume change due to the increase of pressure (S being the section of the sample holder and Δx piston displacement) and m the mass of the sample. Δv_{calib} is a correcting term obtained from calibration tests with degassed, deionized water. This term corrects a systematic error mainly due to a slight deformation of the volumetric device with pressure. The specific volume at high pressure was finally determined with a combined standard uncertainty of $u_c = 1.5 \cdot 10^{-7}$ $m^3 \cdot kg^{-1}$. Since it may be assumed that the possible estimated values of v are approximately normally distributed with the approximate standard deviation u_c, the unknown value of v is believed to lie in the interval $v \pm 2u_c$ with a level of confidence of approximately 95 %.

Calculation of Volumetric Properties

The thermal expansion coefficient, α, and the isothermal compressibility coefficient, k_T, can be calculated from their respective definitions:

$$\alpha = \frac{1}{v}\left(\frac{\partial v}{\partial T}\right)_p \quad \text{and} \quad k_T = -\frac{1}{v}\left(\frac{\partial v}{\partial p}\right)_T \tag{2}$$

On one part, the specific volume was expressed as a function of temperature to be able to calculate the thermal expansion coefficient at atmospheric pressure. On the other part, it was expressed as a function of pressure to obtain the isothermal compressibility at constant temperature.

For the thermal expansion coefficient calculation, the following expression of the specific volume at atmospheric pressure $v_0(T)$ has been used:

$$v_0(T) = v_{00} \exp(C_1 \cdot t + C_2 \cdot t^2) \quad \text{with} \quad t = T - 273.15 \tag{3}$$

where v_{00}, C_1, and C_2 are coefficients to fit, t is the temperature in °C, and T is the temperature in K. This expression was a simplified form of the one proposed by ref 18.

For the isothermal compressibility calculation, the secant bulk modulus equation was selected to express the specific volume as a function of pressure:

$$v(p) = v_0 \frac{B(p) - \Delta p}{B(p)} \quad \text{with} \quad B(p) = B_0 + C_3\Delta p + C_4\Delta p^2 \quad \text{and} \quad \Delta p = p - p_0 \tag{4}$$

v_0 is the specific volume at atmospheric pressure p_0, and $B(p)$ is the secant bulk modulus as a function of pressure, with both

Table 2. Specific Volume of the Studied PTFs at High Pressure

E			EG			PG		
p	T	v	p	T	v	p	T	v
MPa	K	$m^3 \cdot kg^{-1}$	MPa	K	$m^3 \cdot kg^{-1}$	MPa	K	$m^3 \cdot kg^{-1}$
0.1	288.18	0.0012334	0.1	288.22	0.0008954	0.1	288.31	0.0009617
48.4	288.03	0.0011910	49.2	288.19	0.0008811	48.8	288.38	0.0009437
99.1	288.15	0.0011572	99.8	288.18	0.0008684	99.8	288.22	0.0009279
148.8	288.20	0.0011313	149.4	288.18	0.0008577	149.9	288.28	0.0009146
199.1	288.08	0.0011095	199.7	288.21	0.0008479	199.6	288.31	0.0009031
250.2	288.14	0.0010906	249.3	288.19	0.0008392	250.1	288.29	0.0008927
300.5	288.11	0.0010742	299.2	288.18	0.0008312	299.9	288.31	0.0008834
348.4	288.05	0.0010601	349.4	288.15	0.0008238	349.1	288.32	0.0008750
E+W			EG+W			PG+W		
0.1	288.08	0.0010675	0.1	288.13	0.0009105	0.1	288.13	0.0009585
49.2	288.10	0.0010451	49.3	288.33	0.0008968	49.5	288.03	0.0009439
98.3	288.04	0.0010263	100.9	288.36	0.0008842	100.1	288.00	0.0009305
148.4	288.07	0.0010100	149.3	288.33	0.0008737	148.9	288.04	0.0009188
198.9	288.04	0.0009956	199.2	288.31	0.0008639	198.8	287.99	0.0009078
248.3	287.96	0.0009831	251.0	288.32	0.0008545	248.6	288.11	0.0008977
299.9	288.02	0.0009708	300.3	288.33	0.0008464	298.4	288.11	0.0008885
348.5	288.08	0.0009603	348.3	288.33	0.0008391	348.4	288.12	0.0008794
E+W			EG+E			CO		
0.1	298.49	0.0010764	0.1	288.12	0.0009440	0.1	288.22	0.0010383
49.0	298.49	0.0010526	49.4	288.20	0.0009266	48.6	288.15	0.0010159
99.6	298.50	0.0010320	98.2	288.14	0.0009121	99.0	288.11	0.0009971
148.5	298.50	0.0010152	148.2	288.12	0.0008993	148.3	288.12	0.0009821
198.4	298.50	0.0010005	198.4	288.14	0.0008879	199.0	288.13	0.0009685
250.3	298.50	0.0009870	249.1	288.17	0.0008777	249.1	288.11	0.0009569
298.5	298.51	0.0009750	298.3	288.13	0.0008687	299.2	288.11	0.0009467
350.0	298.55	0.0009631	349.5	288.13	0.0008599	349.3	288.10	0.0009374
E+W			SO			CO+E		
0.1	308.42	0.0010854	0.1	288.15	0.0010586	0.1	288.11	0.0011973
49.3	308.38	0.0010606	48.8	288.12	0.0010178	48.6	288.08	0.0011584
99.8	308.39	0.0010393	99.8	288.14	0.0009863	99.5	287.98	0.0011276
148.3	308.39	0.0010219	150.0	288.10	0.0009625	148.3	288.06	0.0011046
198.4	308.45	0.0010061	198.8	288.11	0.0009432	198.5	288.10	0.0010845
248.7	308.47	0.0009922	250.1	288.07	0.0009257	249.5	288.07	0.0010672
298.1	308.45	0.0009798	299.7	288.12	0.0009110	299.0	288.08	0.0010514
349.9	308.46	0.0009680	348.7	288.10	0.0008983	349.1	288.26	0.0010381

magnitudes taken at the temperature of measurement T. B_0 is the bulk modulus at atmospheric pressure, and C_3 and C_4 are coefficients to be fitted. This equation was chosen because of its demonstrated simplicity, suitability, and accuracy in this relatively narrow pressure interval.[13]

Thus, it is finally obtained that:

$$\alpha(T) = C_1 + 2C_2(T - 273.15) \tag{5}$$

and

$$k_T = \frac{B_0 - C_4\Delta p^2}{(C_4\Delta p^2 + C_3\Delta p + B_0)(C_4\Delta p^2 + (C_3 - 1)\Delta p + B_0)} \tag{6}$$

The software TableCurve2D version 5.0 (SPSS Inc., Chicago, IL) has been used to perform the corresponding fittings (Levenberg−Marquardt algorithm).

Results and Discussion

Specific Volume and Thermal Expansion Coefficient at Atmospheric Pressure. The specific volume of the PTFs was measured at atmospheric pressure at each 1 K from (273.15 to 313.15) K. Results are partially shown in Table 2; the complete results can be consulted in the Supporting Information. The specific volume of each PTF increases with temperature. The oil-based PTFs (CO, CO+E, and SO), E, and the E+W mix have a higher specific volume than W; the other PTFs have all a lower one, EG having the lowest. The specific volumes of the E and EG are respectively 1.2 times and 0.9 times that of W at 273.15 K. To understand the differences observed between

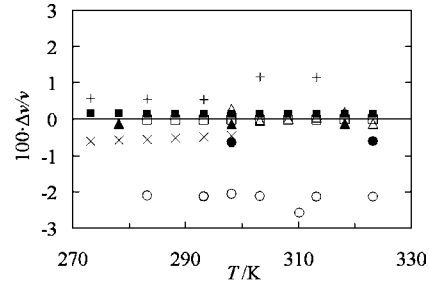

Figure 1. Relative deviations $\Delta v = v(\text{expt.}) - v(\text{lit.})$ between experimental and literature values of the specific volume at atmospheric pressure for the different PTFs: ×, SO ref 21; +, CO ref 34; ○, E ref 44; △, EG ref 45; □, PG ref 47; ●, E+W ref 31; ▲, EG+W ref 14; ■, PG+W ref 36.

the specific volumes of the PTFs, the molecular weights are calculated from the periodic table giving (18, 46, 62, 76, 298, > 310) $g \cdot mol^{-1}$ for W, E, EG, PG, CO (main component: ricinoleic acid), and SO (> dimer), respectively. Thus, the differences observed are less related with the molecular weights of their respective main component than with the interactions between molecules. In this way, W, E, EG, and PG all contain one or two hydroxyl groups which are able to form hydrogen bonds to one another. This is at the root of the relatively high density of W: hydrogen bonds organize water molecules in a quite compact structure. In that way, EG ($C_2H_6O_2$) with two hydroxyl groups also forms a three-dimensional network[29] which is not observed for E (C_2H_5OH) with only one hydroxyl group. E molecules form linear or cyclic aggregates.[39] The structure is probably not so compact for PG ($C_3H_8O_2$) because of the supplementary CH_3 group compared to EG. Besides, PG+W has an unexpected lower specific volume than that of its individual components. This could mean that W molecules, at this concentration (mole fraction = 0.778), are able to organize with PG molecules in a more compact structure than the PG molecules alone. CO and SO are constituted by more complex molecules (triglycerides and polymers, respectively), and they are expected to form more disordered structures than the rest of the studied PTFs. It is likely that their molecules occupy a higher molar volume but with "heavier" molecules leading to intermediate values for the specific volume.

The specific volumes measured are compared with data collected in the literature in Figure 1; comparisons with more references with one figure per PTF can be find in the Supporting Information linked to this article. In the case of the PTF mixtures, the data found in the literature are often expressed in mass or mole units and seldom correspond exactly to the concentration being studied in this paper. Thus, the required conversion and interpolation were performed; the volume concentrations of the studied mixes converted into mass fractions are 0.43, 0.17, 0.55, 0.76, and 0.84 for E+W, CO+E, PG+W, EG+W, and EG+E, respectively (calculated from the measured density data at 298.15 K). The measured specific volumes agree well with the data from literature, showing a relative deviation smaller than 0.2 % on average. The observed deviations can be explained by the different measuring methods used and by the sample degassing or not. For E and E+W, the relative deviations are about 2 % and 0.5 %, respectively. These higher deviations are compatible with the higher purity grade of the ethanol used for the mix by the other authors compared to the one used in this work. The highest differences are found for silicone oil with maximal relative deviations of about 2 % (see Supporting Information). These are attributed to a difference in oil types (the kinematic viscosity claimed by the provider is about 10^{-5} $m^2 \cdot s^{-1}$ for the SO used in this work, see Table 1); in fact, the

Table 3. Fit Coefficients for Equation 3 in the Range of (273.15 to 313.15) K and for Linear Secant Bulk Modulus in Equation 4 in the Range of (0.1 to 350) MPa

	$v_{00}\cdot10^3$	$C_1\cdot10^4$	$C_2\cdot10^6$	r^2	C_3	$C_4\cdot10^3$	B_0	r^2
fluid	$m^3\cdot kg^{-1}$	K^{-1}	K^{-2}	(eq 3)	MPa^{-2}	MPa^{-3}	MPa	(eq 4)
E+W	1.0556	7.2682	1.7376	0.9997				
288.15 K					4.2488	–1.5	2169.0	0.9998
298.15 K					4.3328	–1.6	2044.3	0.9996
313.15 K					4.0537	–1.2	1979.3	0.9999
CO+E	1.1800	9.5504	1.2683	0.9998	4.2676	–1.2	1304.5	1.0000
EG+W	0.9024	5.8017	0.7333	1.0000	4.1501	–1.2	3121.6	0.9998
EG+E	0.9344	6.7534	0.2425	0.9990	4.7856	–1.5	2472.4	0.9998
PG+W	0.9499	5.7845	1.5535	0.9999	4.2416	–1.4	2913.7	0.9999
PG	0.9519	6.5973	1.0917	0.9995	4.6673	–1.4	2338.4	0.9999
SO	1.0431	9.7985	0.0877	1.0000	3.9332	–1.2	1085.7	1.0000
E	1.2143	10.1354	1.4624	0.9999	4.1062	–1.4	1191.0	0.9999
CO	1.0273	6.9799	0.3545	0.9999	4.9237	–1.5	2063.5	0.9999
EG	0.8871	6.1052	0.4236	0.9999	4.6574	–1.2	2896.6	0.9999

relative deviations are about 0.5 % when comparing with a SO of same viscosity.

The experimental results on specific volume at atmospheric pressure were used to fit the coefficients of eq 3, and the values obtained are given in Table 3 for each PTF. Then, the thermal expansion coefficient was calculated as explained in the previous section. The corresponding results are illustrated in Figure 2. The thermal expansion coefficient increases with temperature for all of the PTFs. Its value increases more slowly with temperature than for W, and it is at least twice higher. Unlike for W, the sign of the thermal expansion coefficient does not change even in the case of the water-based PTFs. All of the studied PTFs expanding upon temperature increase in the explored range of temperature. Besides, thermal expansion coefficients of SO and EG+E were almost constant with temperature, meaning that they expand in about the same proportion at "low" and "high" temperatures in the studied temperature range of (273.15 to 313.15) K. A comparison of our data to data found in the literature, only available for SO, CO, E, and PG, shows that the relative deviations did not exceed (5, 2, 1.5, and 0.2) %, respectively (Figure 3a).

Specific Volume and Isothermal Compressibility at High Pressure. The specific volume of the studied PTFs was measured as a function of pressure up to 350 MPa at 288.15 K. In the case of the W+E mix, high-pressure measurements were also performed at (298.15 and 308.15) K. The values obtained in one experiment are shown in Table 2. The values obtained in the other two experiments are provided in the Supporting Information. The specific volume decreases as pressure increases as it was expected. Its value is divided by 1.18 for SO, by 1.17 for E, by 1.15 for CO+E, by 1.12 for W, and by 1.09 to 1.11 for the rest of the PTFs between atmospheric pressure and 350 MPa. The specific volumes of E+W at (288.15, 298.15, and 308.15) K have closer values between each other at 350 MPa than at atmospheric pressure (the differences are reduced by half). The specific volume measured at high pressure are compared to the few data available from the literature for SO, CO, PG, and E+W in Figure 4. These data were previously extrapolated to 288.15 K for SO, CO, and PG and interpolated to a volume fraction of 0.5 for E+W at 298.15 K. The deviations between our measurements and those of the other authors are less than (6, 2, 0.8, and 0.1) % for CO, SO, E+W, and PG, respectively. The deviations for CO and SO are attributable to a difference in raw product characteristics. In the case of E+W, the deviations are related with differences in purity grade.

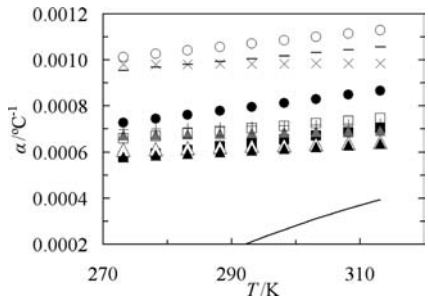

Figure 2. Thermal expansion coefficient of the PTFs as a function of temperature at atmospheric pressure. ×, SO; +, CO; ○, E; △, EG; □, PG; ●, E+W; ▲, EG+W; ■, PG+W; ▲, EG+E; —, CO+E. The curve represents the data of W from ref 21.

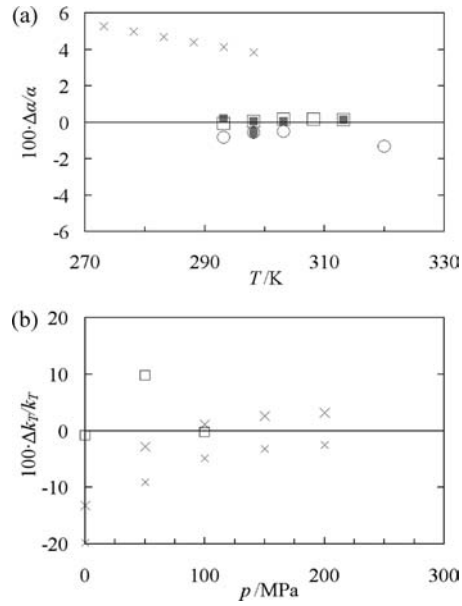

Figure 3. Relative deviations between experimental and literature values for (a) the thermal expansion coefficient: ×, SO ref 30; +, CO ref 34; □, PG ref 47; ■, PG ref 43; ○, E ref 10; ●, E refs 4 and 5; and for (b) the isothermal compressibility: ×, SO ref 38 (two kinematic viscosities: big-sized symbol, $5\cdot10^{-5}$ $m^2\cdot s^{-1}$; small-sized symbol: $3\cdot10^{-6}$ $m^2\cdot s^{-1}$) and □, PG ref 47.

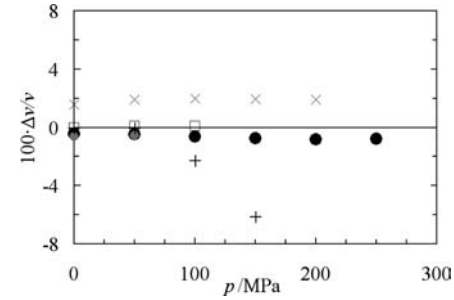

Figure 4. Relative deviations $\Delta v = v(\text{expt.}) - v(\text{lit.})$ between experimental and literature values of the specific volume at high pressure for the different PTFs: ×, SO ref 38; +, CO ref 1; □, PG ref 47; black ●, E+W ref 16; gray ●, E+W ref 31.

The experimental results on specific volume at high pressure were used to fit the coefficients of eq 4, and their values are given in Table 3 for each PTF. Then, the isothermal compressibility was calculated as described in the previous section. The results at 288.15 K are represented as a function of pressure for all of the PTFs in Figure 5. It can be observed that SO, E, and CO+E are the most compressible PTFs, while EG, EG+W and PG+W are the least compressible ones. The isothermal compressibility of SO, E, and CO+E also exhibits a larger variation with pressure than the other PTFs. All of the studied PTFs tend to a similar value of the isothermal compressibility

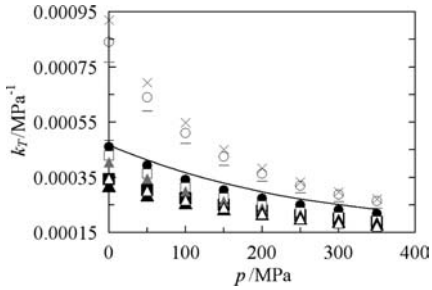

Figure 5. Isothermal compressibility of the PTFs at 288.15 K as a function of pressure. ×, SO; +, CO; ○, E; △, EG; □, PG; ●, E+W; black ▲, EG+W; ■, PG+W; gray ▲, EG+E; —, CO+E. The curve represents the data of W from ref 21.

when increasing the pressure which is comprised between (0.000172 and 0.000271) MPa^{-1} at 350 MPa. The reason of this asymptotic behavior at high pressure is that the free space between molecules is more and more reduced, and volume changes are thus more and more limited. In the case of E+W for which the isothermal compressibility was also determined at (298.15 and 308.15) K, it is observed that k_T increases with temperature and that the corresponding values are more and more different from that of water (data not shown). All of the data obtained could only be compared to values extrapolated at 288.15 K from the data given in ref 38 for SO and in ref 47 for PG: the observed deviations are coarsely around 5 % in both cases (Figure 3b).

Approximation of the Specific Volume and Thermal Expansion Coefficient Behaviors of Mixtures with Pressure and Temperature from That of Their Pure Components. The specific volume and thermal expansion coefficient are used together with the specific heat to calculate the adiabatic heat generated during the compression of a food product. Then the temperature increases, and distribution both in the PTF and in the product can be simulated from heat transfer modeling. Some PTFs are made of a mixture of two or more liquids in variable proportions. Thus, it should be useful to be able to predict the specific volume and thermal expansion coefficient of those PTFs from that of their pure components. The following relationships have been employed by several authors[22,12] to get an approximation of the specific volume v_{mix} of (food components) mixtures at high pressure:

$$v_{mix}(p, T) = x_1 v_1(p, T) + x_2 v_2(p, T) \quad (7)$$

$$v_{mix}(p, T) = \frac{v_{mix}(p_0, T)}{v_1(p_0, T)} v_1(p, T) \quad (8)$$

where x_1 and x_2 are the mass fractions of components 1 and 2 (usually water and dry matter), respectively, and v_1 and v_2 are their specific volumes as a function of pressure and temperature.

In this way, the specific volumes v_{mix} of PG+W, EG+W, EG+E, and CO+E are computed at 288.15 K as a function of pressure from eqs 7 and 8. The specific volume of each pure component is calculated from eq 4 and then introduced in those equations. v_1 is taken as the specific volume of the main component of the mixture in eq 8 (notice that W is not always the main component unlike the case of food). When one of the component is W, the data from ref 21 are employed. Figure 6 shows the experimental versus calculated values of v_{mix} at different pressures. Almost all of the calculated values from eq 7 are higher than the experimental ones. This results from the fact that eq 7 does not take into account the excess molar volume related with the rearrangement between the molecules of the two liquids involved in the mixture. The maximal relative

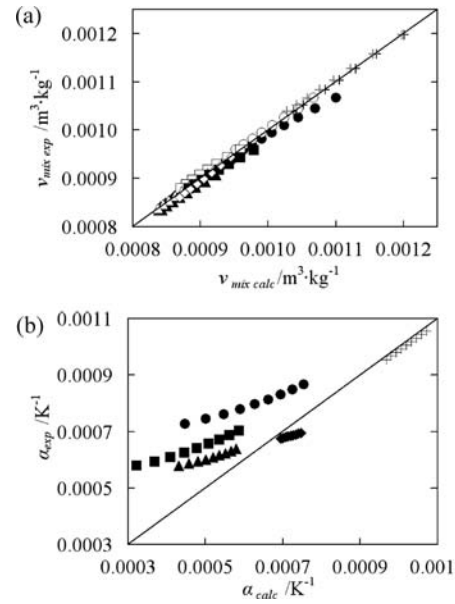

Figure 6. Experimental vs calculated values of (a) specific volume. Dark symbols correspond to the results of eq 7; light symbols correspond to the results of eq 8. (b) Thermal expansion coefficient: ●, E+W; ▲, EG+W; ■, PG+W; ◆, EG+E; +, CO+E.

difference between calculated and experimental values is about 3 % and is observed for E+W at atmospheric pressure. In all cases, this relative difference decreases at higher pressures to less than 0.5 %. In contrast, eq 8 offers better approximations for E+W and EG+W, and the relative differences are generally lower than 1 %. In eq 8, it is implicitly assumed that the ratio between the specific volume of the main component and that of the mixture at atmospheric pressure is maintained at high pressure. Thus, it is not so surprising that the relationship works well at low pressures, but it loses little by little its prediction ability as pressure increases. If water is not the main component but its properties are used, the goodness of the prediction falls drastically; this underlines the importance of knowing the volumetric properties of PTFs other than W.

An approximation of the thermal expansion coefficient of mixtures was calculated by deriving eq 7 and according to eq 2 as detailed below:

$$\alpha_{mix} = \frac{1}{v_{mix}}\left(\frac{\partial v_{mix}}{\partial T}\right)_p = \frac{1}{x_1 v_1 + x_2 v_2}\left(\frac{\partial (x_1 v_1 + x_2 v_2)}{\partial T}\right)_p \quad (9)$$

$$\alpha_{mix} = \frac{1}{x_1 v_1 + x_2 v_2}\left(x_1 v_1 \frac{1}{v_1}\left(\frac{\partial v_1}{\partial T}\right)_p + x_2 v_2 \frac{1}{v_2}\left(\frac{\partial v_2}{\partial T}\right)_p\right) \quad (10)$$

$$\alpha_{mix} = \frac{x_1 v_1 \alpha_1 + x_2 v_2 \alpha_2}{x_1 v_1 + x_2 v_2} \quad (11)$$

Calculations were performed over the whole studied range of temperatures from (273.15 to 313.15) K at atmospheric pressure. The predicted values differed by (16 to 28) % in average from the experimental ones for the water-based PTFs, while the relative difference between predicted and experimental values was only about (1 and 5) % for CO+E and EG+E. It seems that the approximation made was not suitable for water-based PTF probably because of the very peculiar behavior of the pure water thermal expansion coefficient: the prediction error was maximal in the region of low temperature, while it

decreased upon temperature increase. The special packing of water molecules at 277.15 K is disturbed by the presence of other molecules in a more or less strong extent depending on the concentrations of each component. In contrast, the proposed correlation (eq 11) should be useful to approximate the thermal expansion coefficient of nonaqueous mixtures; it remains to check it in the high-pressure range.

Conclusions

From all of the above results, it clearly appears that, even in the case of water-based PTFs, the properties of any PTF cannot be substituted by those of pure water for modeling purposes.

As an alternative to the unavailability of data on PTF mixtures, two relationships based on the properties of its pure components can be employed to predict the specific volume of the mixture. They provide good approximations of the mixture specific volume whatever the considered components and proportions among those studied. The thermal expansion coefficient of a PTF mixture can also be approximated, but the derived relationship only works for the two nonwater-based mixtures EG+E and CO+E. For the other cases, the deviation is related to the anomalous behavior of water thermal expansion coefficient with temperature that can turn "normal" in the presence of other substances.

Supporting Information Available:

A table containing all of the mean values obtained for the specific volume of each PTF at atmospheric pressure between (273.15 and 313.15) K is provided. A set of figures is presented as a complement to Figure 1 of this article. One figure per type of PTF shows the relative deviation between the experimental and the literature values of the specific volume at atmospheric pressure as a function of temperature. SO experimental data are compared to those from refs 21, 27, and 30. CO experimental data are compared to those from refs 1, 32, 34, and 41. EG experimental data are compared to those from refs 14, 35, and 45. PG experimental data are compared to those from refs 17, 36, 43, and 47. E experimental data are compared to those from refs 4, 5, 10, 11, 16, 23, 24, 31, and 44. EG+W experimental data are compared to those from refs 11, 14, 35, and 45. PG+W experimental data are compared to those from refs 11, 17, and 36. E+W experimental data are compared to those from refs 11, 16, 23, 24, and 45. Finally, the other two experimental data sets of specific volume at high pressure are presented in two tables for the different PTFs. This material is available free of charge via the Internet at http://pubs.acs.org.

Literature Cited

(1) Acosta, G. M.; Smith, R. L., Jr.; Arai, K. High-pressure PVT behavior of natural fats and oils, trilaurin, triolein, and n-tridecane from 303 to 353 K from atmospheric pressure to 150 MPa. *J. Chem. Eng. Data* **1996**, *41*, 961–969.

(2) Balasubramanian, S.; Balasubramaniam, V. M. Compression heating influence of pressure transmitting fluids on bacteria inactivation during high pressure processing. *Food Res. Int.* **2003**, *36*, 661–668.

(3) Barbosa-Cánovas, G. V.; Rodríguez, J. J. Thermodynamic aspects of high hydrostatic pressure food processing. In *Novel Food Processing Technologies*; Barbosa-Cánovas, G. V., Tapia, M. S., Cano, M. P., Eds.; CRC Press, Boca Raton, FL, 2005; pp 183−205.

(4) Benson, G. C.; Kiyohara, O. Thermodynamics of aqueous mixtures of nonelectrolytes. I. Excess volumes of water-n-alcohol mixtures at several temperatures. *J. Solution Chem.* **1980**, *9* (10), 791–804.

(5) Benson, G. C.; D'Arcy, P. J. Excess isobaric heat capacities of water-n-alcohol mixtures. *J. Chem. Eng. Data* **1982**, *27*, 439–442.

(6) Buzrul, S.; Alpas, H.; Largeteau, A.; Bozoglu, F.; Demazeau, G. J. Compression heating of selected pressure transmitting fluids and liquid foods during high hydrostatic pressure treatment. *J. Food Eng.* **2008**, *85*, 466–472.

(7) Fuchigami, M.; Teramoto, A. Texture and structure of high-pressure-frozen gellan gum gel. *Food Hydrocolloids* **2003**, *17*, 895–899.

(8) Guignon, B.; Otero, L.; Molina-García, A. D.; Sanz, P. D. Liquid water-ice I phase diagrams under high pressure: Sodium chloride and sucrose models for food systems. *Biotechnol. Prog.* **2005**, *21*, 439–445.

(9) Guignon, B.; Aparicio, C.; Sanz, P. D. Volumetric properties of sunflower and olive oil between 15 and 55°C up to 350 MPa. *High Pressure Res.* **2009**, *29* (1), 38–45.

(10) Hales, J. L.; Ellender, J. H. Liquid densities from 293 to 490 K of nine aliphatic alcohols. *J. Chem. Thermodyn.* **1976**, (8), 1177–1184.

(11) *Handbook of Chemistry and Physics*, 56th ed.; Weast, R. C., Ed.; CRC Press Inc.: Cleveland, OH, 1976.

(12) Hartmann, C.; Delgado, A.; Szymczyk, J. Convective and diffusive transport effects in a high pressure induced inactivation process of packed food. *J. Food Eng.* **2003**, *59*, 33–44.

(13) Hayward, A. T. Compressibility equations for liquids: a comparative study. *Br. J. Appl. Phys.* **1967**, (18), 965–977.

(14) Huot, J.-Y.; Battistel, E.; Lumry, R.; Villeneuve, G.; Lavallee, J.-F.; Anusiem, A.; Jolicoeur, C. A comprehensive thermodynamic investigation of water-ethylene glycol mixtures at 5, 25, and 45 °C. *J. Solution Chem.* **1988**, *17* (7), 601–636.

(15) Koch, H.; Seyderhelm, I.; Wille, P.; Kalichevsky, M. T.; Knorr, D. Pressure-shift freezing and its influence on texture, colour, microstructure and rehydration behaviour of potato cubes. *Nahrung* **1996**, *40* (3), 125–131.

(16) Kubota, H.; Tanaka, Y.; Makita, T. Volumetric behaviour of pure alcohols and their water mixtures under high pressure. *Int. J. Thermophys.* **1987**, *8* (1), 47–70.

(17) MacBeth, G.; Thompson, A. R. Densities and refractive indexes for propylene glycol-water solutions. *Anal. Chem.* **1951**, *23* (4), 618–619.

(18) Mikhailov, G. M.; Mikhailov, V. G.; Reva, L. S.; Ryabchuk, G. V. Precision fitting of the temperature dependence of density and prediction of the thermal expansion coefficient of liquids. *Russ. J. Appl. Chem.* **2005**, *78* (7), 1067–1072.

(19) Min, S.; Sastry, S. K.; Balasubramaniam, V. M. Compressibility and density of selected liquid and solid foods under pressures up to 700 MPa. *J. Food Eng.* **2010**, *96* (4), 568–574.

(20) Otero, L.; Martino, M.; Zaritzky, N.; Solas, N.; Sanz, P. D. Preservation of microstructure in peach and mango during high-pressure-shift freezing. *J. Food Sci.* **2000**, *65* (3), 466–470.

(21) Otero, L.; Molina-Garcia, A. D.; Sanz, P. D. Some interrelated thermophysical properties of liquid water and ice I. A User-friendly modeling review for food high pressure processing. *Crit. Rev. Food Sci.* **2002**, *42* (4), 339–352; http://www.if.csic.es/programas/ifiform.htm.

(22) Otero, L.; Guignon, B.; Aparicio, C.; Sanz, P. D. Modeling thermophysical properties of food under high pressure. *Crit. Rev. Food Sci.* **2009**, *49* (8), 1–25.

(23) Parke, S. A.; Birch, G. G. Solution properties of ethanol in water. *Food Chem.* **1999**, (67), 241–246.

(24) Pečar, D.; Doleček, V. Volumetric properties of etanol-water mixtures under high temperatures and pressures. *Fluid Phase Equilib.* **2005**, (230), 36–44.

(25) Picart, L.; Dumay, E.; Guiraud, J.-P.; Cheftel, J. C. Microbial inactivation by pressure-shift freezing: effects on smoked salmon mince inoculated with Pseudomonas fluorescens, Micrococcus luteus and Listeria innocua. *Lebensm. Wiss. Technol.* **2004**, *37* (2), 227–238.

(26) Rastogi, N. K.; Raghavarao, K. S. M. S.; Niranjan, K.; Knorr, D. Opportunities and challenges in high pressure processing of foods. *Crit. Rev. Food Sci.* **2007**, *47* (1), 69–112.

(27) Ricci, E.; Sangiorgi, R.; Passerone, A. Density and surface tension of dioctylphthalate, silicone oil and their solutions. *Surf. Coat. Technol.* **1986**, (28), 215–223.

(28) Robertson, R. E.; Carroll, T.; Pearce, L. E. Bacillus spore inactivation differences after combined mild temperature and high pressure processing using two pressurizing fluids. *J. Food Protect.* **2008**, *71* (6), 1186–1192.

(29) Rodnikova, M. N.; Chumaevskii, N. A.; Troitskii, V. M.; Kayumova, D. B. Structure of liquid ethylene glycol. *Russ. J. Phys. Chem.* **2006**, *80* (5), 926–930.

(30) Rothgeb, T. M. In *Determination of density and coefficient of thermal expansion of a liquid at low temperature*, A/AA and ASME, 4th Joint thermophysics and heat transfer conference, Boston, MA, June 2−4, 1986.

(31) Safarov, D. T.; Shakhverdiev, A. N. Investigation of the thermophysical properties of ethyl alcohol + water solutions. *High Temp.* **2001**, *39* (3), 424–429.

(32) Sankarappa, T.; Kumar, M. P.; Ahmad, A. Ultrasound velocity and density studies in some refined and unrefined edible oils. *Phys. Chem. Liq.* **2005**, *43* (6), 507–514.

(33) Saowapark, S.; Apichartsrangkoon, A.; Bell, A. E. Viscoelastic properties of high pressure and heat induced tofu gels. *Food Chem.* **2008**, (107), 984–989.

(34) Subrahmanyam, M. S. R.; Sumathi Vedanayagam, H.; Venkatacharyulu, P. Estimation of the sharma constant and thermoacoustic properties of vegetable oils. *J. Am. Oil Chem. Soc.* **1994**, *71* (8), 901–905.
(35) Sun, T.; Teja, A. S. Density, viscosity, and thermal conductivity of aqueous ethylene, diethylene, and triethylene glycol mixtures between 290 and 450 K. *J. Chem. Eng. Data* **2003**, (48), 198–202.
(36) Sun, T.; Teja, A. S. Density, viscosity and thermal conductivity of aqueous solutions of propylene glycol, dipropylene glycol, and tripropylene glycol between 290 and 460 K. *J. Chem. Eng. Data* **2004**, (49), 1311–1317.
(37) Tekác, V.; Cibulka, I.; Holub, R. PVT Properties of Liquids and Liquid Mixtures: a review of the experimental methods and the literature data. *Fluid Phase Equilib.* **1985**, (19), 33–149.
(38) Thern, A.; Lüdemann, H.-D. p, T Dependence of the self diffusion coefficients and densities in liquid silicone oils. *Z. Naturforsch.* **1996**, (51a), 192–196.
(39) Tomšič, M.; Jamnik, A.; Fritz-Popovski, G.; Glatter, O.; Vlček, L. Structural properties of pure simple alcohols from ethanol, propanol, pentanol to hexanol: comparing Monte Carlo simulations with experimental SAXA data. *J. Phys. Chem. B* **2007**, *111*, 1738–1751.
(40) Torres, J. A.; Velasquez, G. Commercial opportunities and research challenges in the high pressure processing of foods. *J. Food Eng.* **2005**, (67), 95–112.
(41) Werner, M.; Baars, A.; Eder, C.; Delgado, A. Thermal conductivity and density of plant oils under high pressure. *J. Chem. Eng. Data* **2008**, (53), 1444–1452.
(42) Wilson, D. R.; Dabrowski, L.; Stringer, S.; Moezelaar, R.; Brocklehurst, T. F. High pressure in combination with elevated temperature as a method for the sterilisation of food. *Trends Food Sci. Technol.* **2008**, (19), 289–299.
(43) Zarei, H. A.; Asadi, S.; Iloukhani, H. Temperature dependence of the volumetric properties of binary mixtures of (1-propanol, 2-propanol and 1,2-propanediol) at ambient pressure (81.5 kPa). *J. Mol. Liq.* **2008**, (141), 25–30.
(44) Zéberg-Mikkelsen, C. K.; Lugo, L.; García, J.; Fernández, J. Volumetric properties under pressure for the binary system ethanol + toluene. *Fluid Phase Equilib.* **2005**, (235), 139–151.
(45) Zhang, J. B.; Zhang, P. Y.; Ma, K.; Han, F.; Chen, G. H.; Wei, X. H. Hydrogen bonding interactions between ethylene glycol and water: density, excess molar volume, and spectral study. *Sci. China, Ser. B: Chem., Life Sci., Earth Sci.* **2008**, *51* (5), 420–426.
(46) Zhu, S.; Le Bail, A.; Chapleau, N.; Ramaswamy, H. S.; De Lamballerie-Anton, M. Pressure shift freezing of pork muscle: effect on colour, drip loss, texture, and protein stability. *Biotechnol. Prog.* **2004**, *20*, 939–945.
(47) Zorebski, E.; Dzida, M.; Piotrowska, M. Study of the acoustic and thermodynamic properties of 1,2- and 1,3-propanediol by means of high-pressure speed of sound measurements at temperatures from (293 to 318) K and pressures up to 101 MPa. *J. Chem. Eng. Data* **2008**, (53), 136–144.

Received for review December 15, 2009. Accepted February 8, 2010. This work has been supported by the "National Plan of Spanish I+D+I MEC" through the projects AGL2007-63314/ALI, CSD2007-00045 Malta Consolider-Ingenio 2010 and to the Madrid Community through the project S2009/PPQ-1551. C.A. and B.G. have a contract from EU and CSIC (I3P and JAE Programs).

JE9010568